

# Searches for supersymmetry in events with photons or tau leptons and missing transverse momentum with the ATLAS detector

---

**Steffen Schaepe\***

On behalf of the ATLAS Collaboration

University of Bonn

E-mail: [schaepe@physik.uni-bonn.de](mailto:schaepe@physik.uni-bonn.de)

Models with gauge-mediated supersymmetry breaking predict that the lightest supersymmetric particle is a gravitino with negligible mass so that the phenomenology of the supersymmetric events produced at the LHC is determined by the next-to-lightest supersymmetric particle (NLSP). Depending on the model parameters, the NLSP can be a neutralino with significant bino admixture that will decay into a photon, or a stau that will decay into a  $\tau$  lepton. The talk presents results from searches for supersymmetry in events with photons or taus and missing transverse momentum, using the data sample recorded in 2011 at  $\sqrt{s} = 7$  TeV center-of-mass energy by the ATLAS experiment at the LHC.

*36th International Conference on High Energy Physics*

*4-11 July 2012*

*Melbourne, Australia*

---

\*Speaker.

## 1. Introduction

Supersymmetry (SUSY) introduces a symmetry between fermions and bosons, resulting in a SUSY partner (sparticle) with identical quantum numbers except a difference by half a unit of spin for each Standard Model (SM) particle. As none of these sparticles have been observed, SUSY must be a broken symmetry if realised in nature. Assuming  $R$ -parity conservation, sparticles are produced in pairs. These would then decay through cascades involving other sparticles until the lightest SUSY particle (LSP), which is stable, is produced.

In gauge-mediated SUSY breaking (GMSB) models, the LSP is the very light (order  $\sim$  keV) gravitino ( $\tilde{G}$ ). The next-to-lightest SUSY particle (NLSP) is the dominant sparticle decaying to the LSP and this leads to experimental signatures which are largely determined by the nature of the NLSP.

In case of a bino-like neutralino NLSP the final decay in the cascade would predominantly be  $\tilde{\chi}_1^0 \rightarrow \gamma\tilde{G}$ , leading to final states with two photons and missing transverse momentum resulting from the undetected gravitinos. A stau NLSP on the other hand leads to final states containing multiple  $\tau$  leptons from the production and decay of the stau and missing transverse momentum from the gravitinos.

This article presents searches for physics beyond the SM in  $\tau$  final states using  $2\text{ fb}^{-1}$  of data and in diphoton final states using  $5\text{ fb}^{-1}$  of data presented in Ref. [1–3] using the ATLAS experiment [4].

Several classes of gauge-mediated models are considered as benchmarks to evaluate the reach of these analysis:

- For the  $\tau$  final states, a minimal GMSB model with full particle spectrum is considered. The SUSY-breaking mass scale  $\Lambda$  and the ratio of the vacuum expectation values of the two Higgs doublets  $\tan\beta$  are treated as free parameters. The other model parameters are fixed to the following values: the messenger mass  $M_{\text{mess}} = 250\text{ TeV}$ , the number of SU(5) messengers  $N_5 = 3$ , the Higgs sector mixing parameter  $\mu > 0$  and the lifetime-parameter  $C_{\text{grav}} = 1$  ensuring prompt NLSP decays ( $c\tau_{\text{NLSP}} < 0.1\text{ mm}$ ).
- The photon search evaluates the SPS8 minimal GMSB model with the only free parameter being the SUSY-breaking mass scale  $\Lambda$ . The other model parameters are fixed to  $M_{\text{mess}} = 2\Lambda$ ,  $N_5 = 1$ ,  $\tan\beta = 15$ ,  $\mu > 0$  and  $C_{\text{grav}} = 1$
- In a general gauge mediation (GGM) simplified SUSY model considered in the photon study the neutralino NLSP, chosen to be the bino, and the gluino masses are treated as free parameters. All other sparticle masses are decoupled, leading to a dominant production mode of a pair of gluinos decaying into the bino-like neutralino NLSP.

## 2. Object reconstruction

Jets, electrons and muons are reconstructed using the standard ATLAS reconstruction for 2011 data.

The missing transverse momentum vector  $\vec{p}_T^{\text{miss}}$  (and its magnitude  $E_T^{\text{miss}}$ ) is measured from the transverse momenta of identified jets, electrons, muons and all calorimeter clusters with  $|\eta| < 4.5$

not associated to such objects. For the purpose of the measurement of  $E_T^{\text{miss}}$ ,  $\tau$  leptons are not distinguished from jets.

The  $\tau$  leptons considered in this search are reconstructed through their hadronic decays. The  $\tau$  reconstruction [5] is seeded from anti- $k_r$  jets ( $R = 0.4$ ) with  $p_T > 10 \text{ GeV}$ . An  $\eta$ - and  $p_T$ -dependent energy calibration to the hadronic  $\tau$  energy scale is applied. Discriminating variables based on track information and observables sensitive to the transverse and longitudinal shape of the energy deposits of  $\tau$  candidates in the calorimeter are used. These quantities are combined in a boosted decision tree (BDT) discriminator to optimize their impact. For these analyses “loose” and “tight” working points have been chosen. Calorimeter information and measurements of transition radiation are used to veto electrons mis-identified as  $\tau$  leptons. Suitable  $\tau$  lepton candidates must satisfy  $p_T > 20 \text{ GeV}$ ,  $|\eta| < 2.5$ , and have one or three associated tracks of  $p_T > 1 \text{ GeV}$  with a charge sum of  $\pm 1$ .

Photon candidates [6] are required to be within  $|\eta| < 1.81$ , and to be outside the transition region  $1.37 < |\eta| < 1.52$  between the barrel and end-cap calorimeters. They are identified on the basis of the characteristics of the longitudinal and transverse shower development in the electromagnetic (EM) calorimeter. In the case that an EM calorimeter deposition is identified as both a photon and an electron, the photon candidate is discarded and the electron candidate retained. Converted photons are re-classified as electrons if one or more candidate conversion tracks included at least one hit from the pixel layers. Giving preference to the electron selection in this way reduced the electron-to-photon fake rate by 50–60% (depending on the value of  $\eta$ ) relative to that of the prior  $1 \text{ fb}^{-1}$  analysis, while preserving over 70% of the signal efficiency. Finally, an “isolation” requirement is imposed. After correcting for contributions from pile-up and the deposition ascribed to the photon itself, photon candidates are removed if more than 5 GeV of transverse energy is observed in a cone of  $\sqrt{(\Delta\eta)^2 + (\Delta\phi)^2} < 0.2$  surrounding the energy deposition in the calorimeter associated with the photon.

### 3. Search in diphoton final states

The data sample for this analysis is selected by a two-photon-trigger. Events are required to contain at least two photon candidates with  $E_T > 50 \text{ GeV}$ .

Three different signal regions (SRs) are defined based on the observed values of  $E_T^{\text{miss}}$ ,  $H_T$ <sup>1</sup> and  $\Delta\phi_{\text{min}}(\gamma, E_T^{\text{miss}})$ <sup>2</sup> (See Table 1).

	SR A	SR B	SR C
$E_T^{\text{miss}} [\text{GeV}] >$	200	100	125
$H_T [\text{GeV}] >$	600	1100	-
$\Delta\phi_{\text{min}}(\gamma, E_T^{\text{miss}}) >$	0.5	-	0.5

**Table 1:** Definition of the three SRs (A, B and C) based on the quantities  $E_T^{\text{miss}}$ ,  $H_T$  and  $\Delta\phi_{\text{min}}(\gamma, E_T^{\text{miss}})$  [3].

<sup>1</sup> $H_T$  is calculated as the sum of the magnitude of the transverse momenta of the selected photons and any additional leptons and jets in the event.

<sup>2</sup> $\Delta\phi(\gamma, E_T^{\text{miss}})$  is defined as the azimuthal angle between the missing transverse momentum vector and either of the two selected photons, with  $\Delta\phi_{\text{min}}(\gamma, E_T^{\text{miss}})$  the minimum value of  $\Delta\phi(\gamma, E_T^{\text{miss}})$  of the two selected photons.

A total of 117, 9 and 7293 candidate events are observed to pass all but the  $E_T^{\text{miss}}$  requirement of SR A, B and C, respectively. After imposing the final  $E_T^{\text{miss}}$  requirement, no events remained for SR A and B, while two events remained for SR C.

Figure 1 shows the  $H_T$  distribution of selected diphoton events, with those of the signal models overlaid.

The contribution to the large  $E_T^{\text{miss}}$  diphoton sample from SM sources can be grouped into three primary components. Those having a fake  $E_T^{\text{miss}}$  due to mis-measured jet and either true photons or photons faked by jets are referred to as ‘‘QCD background’’. Contributions with true  $E_T^{\text{miss}}$  from neutrinos in the final state and either jets or electrons mis-reconstructed as photons are referred to as ‘‘EW background’’. The third background component, referred to as ‘‘irreducible’’, consists of  $W$  and  $Z$  bosons produced in association with two real photons, with a subsequent decay into one or more neutrinos.

To estimate the QCD background a dedicated control sample has been selected having one of the two photons likely to be faked by another object. An estimate of the QCD background contamination in each SR is obtained from imposing the  $E_T^{\text{miss}}$  requirement associated with the given SR upon the corresponding QCD template, after normalising each template to the diphoton data with  $E_T^{\text{miss}} < 20\text{GeV}$  from the given SR.

An alternative estimate has been applied to SRs A and B by gradually raising the  $H_T$  cut on the QCD templates and extrapolating from lower  $H_T$  cuts into the SR. Differences between the two approaches are accommodated as systematic uncertainties.

The EW background, is estimated via a control sample composed of events with at least one photon and one electron, each with  $E_T > 50\text{GeV}$ , and scaled by the probability for an electron to be mis-reconstructed as a photon, Systematic uncertainties are dominated by uncertainties on the fake factors and ambiguities between different sources of mis-reconstructed photons.

	SR A	SR B	SR C
QCD	$0.07 \pm 0.00 \pm 0.07$	$0.27 \pm 0.00 \pm 0.27$	$0.85 \pm 0.30 \pm 0.71$
Electroweak	$0.03 \pm 0.03 \pm 0.01$	$0.09 \pm 0.05 \pm 0.02$	$0.80 \pm 0.16 \pm 0.22$
$W(\rightarrow \ell\nu) + \gamma\gamma$	$< 0.01$	$< 0.01$	$0.18 \pm 0.13 \pm 0.18$
$Z(\rightarrow \bar{\nu}\nu) + \gamma\gamma$	$< 0.01$	$< 0.01$	$0.27 \pm 0.09 \pm 0.04$
Total	$0.10 \pm 0.03 \pm 0.07$	$0.36 \pm 0.05 \pm 0.27$	$2.11 \pm 0.37 \pm 0.77$
Observed events	0	0	2

**Table 2:** The expected number of  $\gamma\gamma$  events for each of the three signal regions including statistical and systematic uncertainties [3].

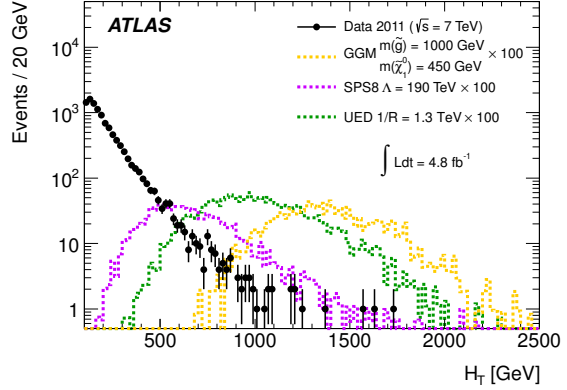


**Figure 1:** The  $H_T$  spectrum of  $\gamma\gamma$  candidate events in the data together with the spectra from simulated signal samples after the diphoton requirement. The signal samples are scaled by a factor of 100 for clarity [3].

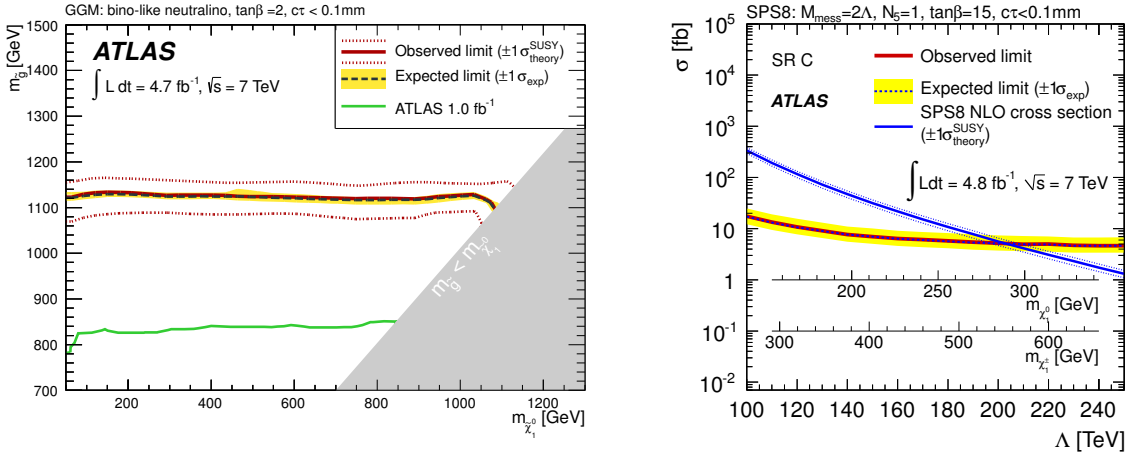


**Figure 2:** Expected and observed 95 % CL lower limits on the gluino mass as a function of the neutralino mass in the GGM model with a bino-like lightest neutralino NLSP (left plot) and on the sparticle production cross section in the SPS8 model, and the NLO cross-section prediction, as a function of  $\Lambda$  and the lightest neutralino and chargino masses (right plot) [3].

The contribution of the irreducible background from the  $Z(\rightarrow \nu\bar{\nu}) + \gamma\gamma$  and  $W(\rightarrow \ell\nu) + \gamma\gamma$  processes is estimated using MC samples. All estimates, along with the resulting estimates for the total background from all sources, are reported in Table 2.

No evidence for physics beyond the SM is observed in any of the SRs. Based on the numbers of observed events in SR A, B and C and the background expectation shown in Table 2, 95 % Confidence Level (CL) upper limits are set on the numbers of events in the different SRs from any scenario of physics beyond the SM using the profile likelihood and  $CL_s$  prescriptions. Uncertainties on the background expectation are treated as Gaussian-distributed nuisance parameters in the maximum likelihood fit, resulting in observed upper limits of 3.1, 3.1 and 4.9 events for SRs A, B and C, respectively.

Limits are also set on the GGM gluino mass as a function of the bino-like neutralino mass, making use of the SR (A or B) that provides the most stringent expected limit for the given neutralino mass (Figure 2). For comparison the lower limits on the GGM gluino mass from an earlier analysis based on 1 fb<sup>-1</sup> from 2011 are also shown.

Including all sources of uncertainty other than the theoretical uncertainty, 95 % CL upper limits on the cross section of the SPS8 model are derived from the SR C result and displayed in Fig. 2 for the range  $\Lambda = 100\text{--}250$  TeV along with the overall production cross section and its theoretical uncertainty. For illustration the cross-section dependence as a function of the lightest neutralino and chargino masses is also shown.

#### 4. Search in $\tau$ final states

Candidate events are pre-selected by a trigger requiring a hard leading jet and large missing transverse momentum translating into requirements of a leading jet with  $p_T > 130$  GeV and  $E_T^{\text{miss}} > 130$  GeV.

Pre-selected events are then required to have at least one “tight” or two “loose”  $\tau$  candidates respectively, and must not contain any electron or muon candidates. To suppress soft multi-jet events, a second jet with  $p_T > 30\text{ GeV}$  is required.

Remaining multi-jet events are rejected by requiring the azimuthal angle between the missing transverse momentum and either of the two leading jets  $\Delta\phi(\vec{p}_T^{\text{miss}}, \text{jet}_{1,2})$  to be larger than 0.4 rad. For the  $1\tau$  channel an additional suppression is achieved requiring the ratio of missing transverse momentum to effective mass<sup>3</sup>  $m_{\text{eff}}/E_T^{\text{miss}} > 0.25$ .

To SRs are defined for the one and  $2\tau$  search respectively requiring  $m_{\text{eff}} > 600/700\text{ GeV}$ . Additionally the transverse mass<sup>4</sup> of the  $\tau$  candidate is required to be larger 110 GeV in the  $1\tau$  case while for the  $2\tau$  search the sum of the transverse masses of both candidates is required to be  $m_T^{\tau_1} + m_T^{\tau_2} > 80\text{ GeV}$ .

The dominant backgrounds arise from top-pair plus single top events (here generically indicated as  $t\bar{t}$ ) and  $W \rightarrow \tau\nu_\tau$  events. For the  $1\tau$  search taus can both be real or come from mis-measured jets while the  $2\tau$  backgrounds comprise final states with one real  $\tau$  and one mis-reconstructed  $\tau$  candidate. Background contribution from  $t\bar{t}$  and  $W \rightarrow \tau\nu_\tau$  are determined in dedicated control regions (CRs) constructed to contain minimal contribution of potential signal and other background sources. The MC overestimates the number of events in the CR compared to data, due to mis-modeling of  $\tau$  misidentification probabilities. MC studies show that the  $\tau$  misidentification probability is, to a good approximation, independent of  $m_{\text{eff}}$ , so that the measured ratio of the data to MC event yields in the CR can be used to correct the MC background prediction in the SR.

Background contributions from multijet events are also estimated from data using looser  $\tau$  requirements and extrapolating to the ones used in the analysis. All other backgrounds are taken from Monte Carlo simulations.

	$t\bar{t}$	W + jets	Z + jets	Multi-jet	$\Sigma\text{SM}$	Data
$1\tau$	$5.6 \pm 1.4$	$4.7 \pm 1.5$	$2.4 \pm 0.7$	$0.5 \pm 0.6$	$13.2 \pm 4.2$	11
$2\tau$	$1.6 \pm 0.9$	$2.5 \pm 1.6$	$1.1 \pm 0.9$	$< 0.01$	$5.3 \pm 2.6$	3

**Table 3:** Expected number of background events for the signal regions of both the  $1\tau$  and the  $2\tau$  search. Uncertainties consist contributions from limited Monte Carlo statistics, limited data statistics in the control regions and instrumental systematic uncertainties.

<sup>3</sup>The effective mass  $m_{\text{eff}}$  is calculated as the sum of  $E_T^{\text{miss}}$  and the magnitude of the transverse momenta of the two highest- $p_T$  jets and all selected taus.

<sup>4</sup>The transverse mass  $m_T$  formed by  $E_T^{\text{miss}}$  and the  $p_T$  of the  $\tau$  lepton is defined as  $m_T = \sqrt{2p_T^\tau E_T^{\text{miss}}(1 - \cos(\Delta\phi(\tau, \vec{p}_T^{\text{miss}})))}$ .

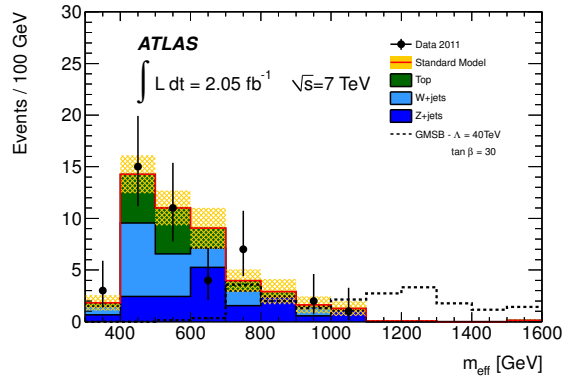


**Figure 3:**  $m_{\text{eff}}$  distribution after the  $\Delta\phi(\vec{p}_T^{\text{miss}}, \text{jet}_{1,2})$  requirement for the  $2\tau$  channel [2].

Dominant uncertainties on the estimated backgrounds arise from the extrapolation uncertainty of the data driven methods, the uncertainty on the jet and  $\tau$  energy scales as well from limited data and Monte Carlo statistics. Table 3 lists all backgrounds with their uncertainties.

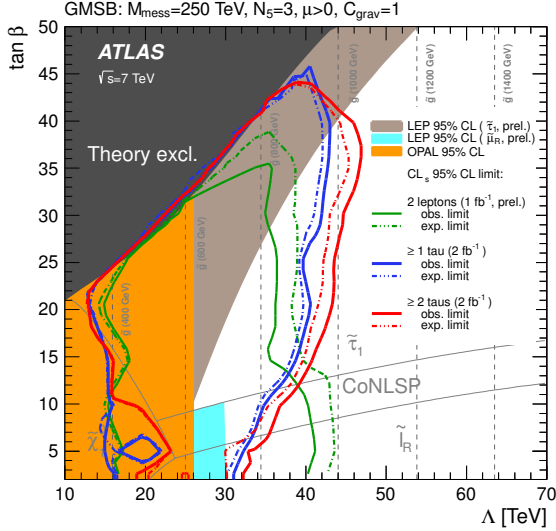


**Figure 4:** Expected and observed 95 % CL lower limits on the minimal GMSB model parameters  $\Lambda$  and  $\tan\beta$ . The limits from the OPAL experiment are shown for comparison [7].

Based on the observation of 11 (3) events in the signal regions an upper limit of 8.5 (7) events is set at 95 % CL on the number of events from any scenario of physics beyond the SM for the  $1\tau$  ( $2\tau$ ) final state, using the profile likelihood and  $CL_s$  method. Uncertainties on the background and signal expectations are treated as Gaussian-distributed nuisance parameters in the likelihood fit. The resulting expected and observed 95 % CL limits on the GMSB model parameters  $\Lambda$  and  $\tan\beta$  are shown in Fig. 4. These limits are calculated including all experimental and theoretical uncertainties on the background and signal expectations. Excluding the theoretical uncertainties on the signal cross section from the limit calculation has a negligible effect on the limits obtained.

Using the correspondence of  $\Lambda$  with the gluino mass a limit of  $m_{\tilde{g}} > 920(990)$  GeV for  $\tan\beta > 20$  can be set for the  $1\tau$  ( $2\tau$ ) channel.

## References

- [1] ATLAS Collaboration, *Search for Supersymmetry with Jets, Missing Transverse Momentum and at Least One Hadronically Decaying Tau Lepton in Proton-Proton Collisions at  $\sqrt{s}=7$  TeV with the ATLAS Detector*, *Phys. Lett.* **B 714** (2012) 197 [1204.3852].
- [2] ATLAS Collaboration, *Search for Events with Large Missing Transverse Momentum, Jets and at Least Two Tau Leptons in 7 TeV Proton-Proton Collision Data with the ATLAS Detector*, *Phys. Lett.* **B 714** (2012) 180 [1203.6580].
- [3] ATLAS Collaboration, *Search for diphoton events with large missing transverse momentum in 7 TeV proton-proton collision data with the ATLAS detector*, 1209.0753.
- [4] ATLAS Collaboration, *The ATLAS Experiment at the CERN Large Hadron Collider*, *J. Instrum.* **3** (2008) S08003.
- [5] ATLAS Collaboration, *Performance of the Reconstruction and Identification of Hadronic Tau Decays with ATLAS*, . <http://cdsweb.cern.ch/record/1398195>.
- [6] ATLAS Collaboration, *Measurement of the inclusive isolated prompt photon cross section in pp collisions at  $\sqrt{s} = 7$  TeV with the ATLAS detector*, *Phys. Rev.* **D83** (2011) 052005 [1012.4389].
- [7] ATLAS Collaboration. <https://atlas.web.cern.ch/Atlas/GROUPS/PHYSICS/PAPERS/SUSY-2011-16/>, April, 2012.